

Suitability of static yield stress evolution to assess thixotropy of flowable cementitious materials

ABSTRACT

Behavior of self-consolidating concrete (SCC) after casting (such as stability, formwork pressure, and multi-layer interfaces) is directly affected by the flocculation aspect of thixotropy. The main objective of this paper is to evaluate the suitability of considering the evolution of static yield stress (τ_0) over time in order to assess the magnitude of thixotropy. Three series of highly flowable mortar mixtures are tested using the four-bladed vane method, and results compared to the cohesion (C) values obtained by direct shear. Test results have shown that τ_0 and C responses determined at given resting time are quite close to each other, which resulted in adequate correlation between thixotropy determined by vane and direct shear methods. This reflects the suitability of considering the evolution of τ_0 over time to quantify the flocculation aspect of thixotropy, as well as its robustness as it is not affected by the testing method.

Keywords: Fresh concrete, Thixotropy, Four-bladed vane, Direct shear test.

INTRODUCTION

The successful casting of highly flowable self-consolidating concrete (SCC) entails proper knowledge and monitoring of thixotropic properties. For instance, the cementitious matrix should be easily deflocculated during agitation with reduced apparent viscosity, thus facilitating placement by gravity with improved passing ability [1,2]. As soon as SCC placement is completed, the reversible phenomenon associated with the build-up of cementitious structure takes place over time. In vertical elements, a fast recovery is required

25 as this improves stability and resistance towards aggregate segregation. Earlier studies
26 showed that lack of stability can lead to surface defects, including bleeding and settlement
27 that can weaken the quality of interface between aggregate and cement paste with direct
28 effects on permeability, bond to steel, and mechanical properties [3,4]. Also, fast
29 restructuring could be beneficial to reduce the SCC lateral stresses developed vertical
30 formworks [5].

31 In contrast, excessively high thixotropic SCC may not be appropriate when casting is made
32 using injection or pumping techniques; i.e., if the material builds-up its internal structure too
33 fast and apparent yield stress exceeds a critical value, any stoppage (such as due to
34 replenishment of buckets) may cause blockage of pipes and eventually abuse the equipment
35 ultimate pressure in order to resume placement [1,2]. Also, high thixotropic SCC exhibiting
36 fast structural recovery could not be appropriate during multi-layers casting in horizontal
37 elements, as this creates cold joints and weak interfaces in the final structure. Some
38 researchers reported mechanical and bond losses reaching 60% due to weak SCC interfaces
39 [6,7].

40 Thixotropy of cementitious materials is often quantified by measuring the surface area during
41 successive shear rate vs. stress measurements (Fig. 1). For example, because of the thixotropy
42 transient and time-dependent nature, hysteresis loops are created when the plastic material is
43 subjected to successive increasing/decreasing shear rates [1,2,5]. During the increasing ramp,
44 de-flocculation occurs but not fast enough for a steady state stress to be reached. The
45 measured stress is thus higher than what would be obtained if steady state was reached.
46 During the decreasing ramp, flocculation occurs but again not fast enough for steady state to
47 be reached, which creates the so-called hysteresis loops. Alternately, thixotropy can be
48 quantified using the structural breakdown curves determined by subjecting the fresh material
49 to given shear rate and recording stress variations over time [5]. The curves are typically

50 characterized by peak yield stress that corresponds to the initial structural condition, and
 51 stress decay towards an equilibrium value (Fig. 1). Nevertheless, it is important to note that
 52 surface areas determined under dynamic conditions (i.e., hysteresis and structural breakdown
 53 curves) are highly dependent on the type of rheometer and testing protocol including applied
 54 shear rate and flow history [2]. This prevents inter-laboratory comparison of test results and
 55 renders difficult the assessment of concrete properties using standardized testing protocols.

56 Given the concrete static condition when placement is completed, several authors studied the
 57 evolution of static yield stress (τ_0) over time [8,9,10], which would reflect the flocculation
 58 aspect of thixotropy and could be more relevant when assessing SCC behavior after casting
 59 such as stability, formwork pressure, and multi-layer interfaces. The τ_0 is defined as the
 60 minimum stress required to initiate flow [11]; it reflects the physical restructuring of inter-
 61 particles links following a rest period coupled with attractive forces due to chemical reactions
 62 and formation of hydration compounds. The vane method is commonly used for measuring
 63 τ_0 , because of its simplicity and possibility of preventing slip during shearing [2,5,9]. Its
 64 principle consists of inserting a four-bladed vane of diameter (D) and height (H) in the plastic
 65 material and recording at sufficiently low shear rate the maximum torque (T_m) required to
 66 initiate flow. Considering the top edges of blades vane aligned with upper material surface
 67 (i.e., to eliminate over-head stress contribution on torque measurements) and yielding
 68 occurring at the cylindrical surface defined by the blade tips [11,12], T_m can be written as:

$$69 \quad T_m = \left(\frac{\pi D^3}{2}\right) \left(\frac{H}{D} + \frac{1}{6}\right) \tau_0 \quad \text{Eq. 1}$$

70 When measurements are made at successive elapsed resting times after initial concrete
 71 mixing, τ_0 was found to increase linearly over time, which could be associated with the
 72 structuration rate of the cementitious matrix, following Eq. 2:

$$73 \quad \tau_0(t_{\text{rest}}) = \tau_0(t_0) + A_{\text{Thix}} t_{\text{rest}} \quad \text{Eq. 2}$$

74 where t_{rest} is the resting time and A_{Thix} structuration rate (i.e., reflecting the magnitude of

75 thixotropy) in Pa/s determined as the slope of tendency curve plotted between $\tau_0(t_{rest})$ and t_{rest} .

76 **USE OF DIRECT SHEAR TO ASSESS THIXOTROPY**

77 The direct shear test is widely used in soil mechanics to determine shear strength properties
78 and analyze failure mechanisms occurring along interfaces. Its principle is quite simple, and
79 consists of shearing two portions of a specimen by the action of steadily increasing force
80 while constant load is applied normal to the plane of relative movement. Shear strength
81 including cohesion (C) and angle of internal friction (ϕ) follow the Mohr-Coulomb law, given
82 as:

$$83 \quad \tau = C + \sigma' \tan \phi \quad \text{Eq. 3}$$

84 where τ and σ' refer to shear resistance and normal effective stress resulting from the solid
85 grains, respectively.

86 In literature, the direct shear has often been employed as a reference test to develop and
87 validate constitutive models characterizing the yield behavior of plastic materials. In fact, this
88 test is standardized under ASTM D3080 [13] and available in most research centers; it is
89 realized under quasi-static conditions whereby shearing takes place within the material along
90 pre-defined interface represented by the horizontal surface area of shearing box. This
91 physically overcomes the complications related to wall slip, secondary flow, and confinement
92 conditions encountered in conventional rheometers [2,12,14]. Alfani and Guerrini [15]
93 reported that direct shear is particularly suited for rheological characterization and interfacial
94 flow behavior between extrudable cohesive pastes and equipment forming wall systems. Lu
95 and Wang [16] considered the direct shear test to validate a constitutive model developed for
96 predicting yield stress of cementitious materials. The C determined by direct shear was found
97 to be closely related with the “true” τ_0 determined at low rotational speed using the four-
98 bladed vane [10]. Recently, Assaad et al. [12] used the direct shear test to validate the effect
99 of vane positioning on τ_0 responses of freshly mixed cement pastes and poly-vinyl acetate

100 emulsions possessing different flowability levels. Over-estimation of τ_0 occurred when the
101 vane was inserted inside the specimen, particularly for cohesive materials. Conversely,
102 positioning the vane blades flush with the upper specimen surface eliminated the contribution
103 of material self-weight on torque measurements and resulted in close C and τ_0 values [12].

104 This paper is part of a comprehensive research project undertaken to provide new insights on
105 various approaches used to quantify thixotropy of cementitious materials. It does not aim at
106 substituting the vane method by direct shear, especially knowing that the vane method is
107 widely used, simple, and versatile. Rather, the main objective of this paper is to evaluate the
108 suitability and robustness of considering the evolution of τ_0 over time determined by vane
109 method in order to quantify the magnitude of thixotropy. Three series of highly flowable
110 mortar mixtures are tested using the vane method, and results compared to those obtained by
111 direct shear. Data presented in this paper can be of interest to researchers in various industries
112 to facilitate inter-laboratory comparison and unify quantification of the flocculation aspect of
113 thixotropy using standardized testing protocols.

114 **EXPERIMENTAL PROGRAM**

115 **1-Materials**

116 Portland cement and silica fume conforming to ASTM C150 Type I and C1240, respectively,
117 are used. The surface areas of cement (Blaine) and silica fume (B.E.T.) were 340 and 20,120
118 m^2/kg , respectively; their specific gravities were 3.14 and 2.22, respectively. Continuously
119 graded siliceous sand complying with ASTM C33 specification was employed; its nominal
120 particle size, fineness modulus, and bulk specific gravity were 4.75 mm, 2.42, and 2.63,
121 respectively.

122 A polycarboxylate-based high-range water reducer (HRWR) complying with ASTM C494
123 Type F was incorporated in all mixtures. It had a specific gravity, solid content, alkali
124 content, and pH of 1.1, 42%, 0.34%, and 6.2, respectively.

125 Liquid viscosity-modifying admixture (VMA) and thixotropy-enhancing agent (TEA) were
126 used. The VMA is based on hydroxyethyl cellulose (HEC) ether with a specific gravity and
127 solid content of 1.04 and 18%, respectively. It is commonly used for SCC production, with
128 recommended dosage rates varying from 0.15% to 1% of cement mass. This VMA is
129 produced by substituting number of hydroxyl groups within the cellulose backbone by
130 functional groups to improve water solubility through a decrease in the molecule crystallinity.
131 Its average weight molecular mass and degree of substitution are equal to 310 kDa and 1.8,
132 respectively.

133 The TEA is an organic cyclic propylene carbonate (PC) compound produced from propylene
134 oxide and carbon dioxide with a zinc halide catalyst. Its specific gravity and pH are 1.03 and
135 6.5, respectively, and recommended dosage for cement-based materials varies from 0.2% to
136 1.2% of cement mass. As will be discussed later, the use of TEA was necessary to increase
137 the magnitude of A_{Thix} beyond 1 Pa/s; in fact, increasing the HEC-based VMA concentration
138 to achieve higher thixotropic level is accompanied with considerably increased HRWR
139 molecules to maintain similar flowability, thus delaying cement hydration reactions and
140 extending setting times beyond 24 hours [17,18]. Conversely, the delay in setting time was
141 limited when the PC-based TEA was used in conjunction with HRWR.

142 **2-Mixture proportioning**

143 Three mortar series proportioned with cement varying from 375 to 435 and 500 kg/m³ and
144 water-to-cement ratio (w/c) from 0.46 to 0.41 and 0.34, respectively, are considered (Table
145 1). The mixtures were proportioned using the concrete-equivalent-mortar (CEM) approach;
146 i.e., the cement content and w/c remained similar to those of corresponding concrete, except
147 that all coarse aggregates are replaced by an equivalent quantity of sand in terms of specific
148 surface area [19,20]. Aggregate-free CEM mixtures could better reflect the flocculation
149 aspect of thixotropy, given that aggregates mostly affect internal friction that overshadows

150 the build-up phenomenon of cementitious matrix [5,20].

151 In total, 12 CEM mixtures are tested. The silica fume, VMA, and TEA were added at
152 relatively low to high dosage rates to achieve different A_{Thix} levels; i.e. silica fume at 5% or
153 10%, VMA at 0.35% or 0.8%, and TEA at 0.3% or 0.75% of cement mass (Table 1). In all
154 mortars, the HRWR was adjusted to secure a flow of 220 ± 10 mm when determined as per
155 ASTM C1437 (this flow corresponds to concrete slump flow of 650 ± 20 mm determined
156 using ASTM C143 slump cone) [21].

157 **3-Mixing and stability testing**

158 The mortar mixing procedure consisted of homogenizing the sand with half of mixing water,
159 then introducing the cementitious materials gradually over 30 seconds. The remaining part of
160 water along with the VMA or TEA along with HRWR were then added and mixed for 1.5
161 minutes. After a rest period of 30 seconds, the mortar was remixed for 1.5 additional minutes.
162 Testing and sampling were made at room temperature of 23 ± 2 °C and $50\% \pm 5\%$ relative
163 humidity.

164 Right after mixing, the flow was measured by determining the material's average diameter
165 after spreading on horizontal surface using a mini-slump cone having top diameter, bottom
166 diameter, and height equal to 70, 100, and 50 mm, respectively [14]. The passing ability was
167 evaluated using the Marsh cone having 12.7-mm outlet diameter; a volume of 500-mL was
168 filled in the cone and allowed to rest for 5 seconds prior to flow time measurement. The
169 bleeding was determined as per ASTM C232, and consists of measuring the relative quantity
170 of mixing water that has bled from the fresh material placed in 75-mm diameter and 150-mm
171 height container. For measurements, the container was slightly tilted and free water collected
172 using a pipet from the specimen surface. The percentage of bleed water was obtained by
173 dividing the collected water by the total mixing water in specimen.

174

175 4-Assessment of τ_0 using the four-bladed vane

176 Right after mixing, the mortars were placed in 5 separate cylindrical recipients having each
177 120-mm height and 100-mm diameter for τ_0 measurements at 5 different t_{rest} intervals (i.e., at
178 0, 20, 40, 60, and 80 min). Anton Paar rheometer connected to four-bladed vane having 24-
179 mm height and 12-mm diameter was used. For each measurement realized at given t_{rest} , the
180 vane was gently introduced in the mortar in a way to position the top vane edges aligned with
181 the upper material's surface. This was found particularly important when testing was realized
182 at longer t_{rest} intervals of relatively moderate to high thixotropic mortars, as this avoided the
183 material disturbance during the vane insertion process. It is to be noted that, prior to vane
184 insertion, care was taken to tilt the recipient gently in order to remove using a pipette the
185 eventual bleed water that occurred during the rest period (all mortars filled in recipients were
186 covered by wet burlap during the rest period). The testing protocol consisted on subjecting
187 the mortar to very low rotational speed of 0.3 rpm and recording the changes in torque as a
188 function of time (mortars tested at t_0 were allowed to rest for 1 min prior to testing).

189 5-Assessment of C by direct shear

190 An ELE Direct Shear apparatus complying with ASTM D3080 [13] was used for measuring
191 C values of tested CEM (Fig. 2). The metal shear box measuring 100 mm diameter and 58
192 mm height is divided into two halves horizontally; the lower section can move forward at
193 different constant velocities varying from 0.001 to 9 mm/min, while the upper section
194 remains stationary. In order to eliminate friction between the two sections during movement
195 and allow C measurements in the order of few Pa, four perfectly aligned 10-mm long
196 channels were laser-grooved in the bottom part of the shear box [15]. A steel ball having 2.5-
197 mm diameter was then placed in each channel, thus allowing the lower plate of the shear box
198 to behave like a roller with respect to the upper plate. The gap between both plates was 10 ± 1
199 μm , and filled with grease to avoid material's leakage. The shear stresses were calculated by

200 dividing the horizontal load by the specimen's cross-sectional area, i.e. 7850 mm^2 . The
201 complete description of direct shear test used can be seen in reference 12.

202 After mixing, the mortar was filled in the shear box and allowed to rest for the specified time
203 interval (a new mortar was batched for each test). To alleviate the experimental program, 3
204 tests at different t_{rest} were realized for each mortar, except the 0.46-5%SF and 0.41-5%SF
205 mortars where 4 tests are conducted. The displacement rates were fixed at 0.5 mm/min, a
206 value found experimentally enough to overcome the restoring forces due to reorientation of
207 particles and structural development due to cement hydration [12]. It is to be noted that the ϕ
208 parameter was not determined in this study, given that testing was realized without normal
209 load applied on top of specimen during the shearing process.

210 TEST RESULTS AND DISCUSSION

211 1-HRWR demand, setting times, and stability testing

212 Table 2 summarizes the HRWR dosage needed to achieve flow of 220 ± 10 mm along with
213 the resulting unit weight, setting time, and stability indexes used to characterize CEM
214 behavior. Briefly, the HRWR demand increased when mortars contained higher silica fume
215 or VMA concentration. The increase in HRWR/VMA lengthened the setting time due to
216 higher molecules adsorption onto cement particles that partly blocks the hydration reactions
217 [17]. For example, the setting was delayed from 9:30 to 10:15 and 14:15 hr:min for 0.46-
218 5%SF, 0.46-10%SF, and 0.46-0.8%VMA, respectively. Mixtures containing TEA exhibited
219 remarkably reduced setting times, as compared to equivalent mortars made with VMA.

220 As summarized in Table 2, the unit weights varied from 1920 ± 15 to 2050 ± 30 and 2140 ± 20
221 kg/m^3 for mixtures made with 0.46, 0.41, and 0.34 w/c, respectively. Generally speaking, the
222 flow time increased with the reduction of w/c, particularly with the addition of silica fume or
223 VMA, given the increased inter-particle friction and cohesiveness [2,3]; values varied from
224 38 to 90 sec. Mortars incorporating TEA exhibited relatively moderate flow times of 73 sec,

225 given that the mixture was not allowed to rest and build its structure prior to testing [17,18].
226 Typical variations in cumulative bleeding over time for selected mortars are given in Fig. 3.
227 Depending on CEM composition, the bleed water increased at different rates during the initial
228 20-min after placement, and tended to stabilize thereafter. For example, the bleeding rate
229 decreased from 0.353 to 0.125 and 0.065 %/min for the 0.46-5%SF, 0.41-10%SF, and 0.34-
230 0.35%VMA, respectively; the corresponding maximum bleed water determined after
231 stabilization was 10.3%, 3.3%, and 1.5%, respectively. The 0.34-0.75%TEA mortar exhibited
232 the lowest bleed rate and stabilized value, given its fast restructuring. Table 2 summarizes the
233 bleeding rates determined over the initial 20-min and maximum bleed values obtained after
234 stabilization.

235 **2-The τ_0 and C responses – Repeatability of testing**

236 Typical shear stress vs. horizontal displacement curves obtained by direct shear for selected
237 mortars at different t_{rest} intervals are given in Fig. 4. As can be seen, the shear stress profiles
238 showed linear elastic region until reaching the maximum peak value (taken as C). The
239 presence of maximum value is an index of flocculation aspect of thixotropy that can be
240 explained by the concept of structural build-up of bonds in the flocculated system [9,11,12].
241 Further horizontal displacement causes the stresses to decrease towards a steady state region.
242 At maximum shear value, the horizontal displacement of bottom shear box varied from 1 to 3
243 mm, depending mostly on t_{rest} interval. It is to be noted that the direct shear profiles are very
244 similar to those typically obtained using the four-bladed vane [11,12,16], which reflects the
245 similarity of both testing methods. The τ_0 and C values determined at various resting intervals
246 are summarized in Table 3.

247 In order to evaluate repeatability of testing, three selected mortars possessing low to high
248 thixotropic levels were tested 3 times using the vane and direct shear methods (a new batch
249 was considered for each test). The coefficients of variation (COV) calculated as the ratio

250 between standard deviation of responses and their mean values, multiplied by 100, are shown
251 in Fig. 5. Generally speaking, the moderately thixotropic mixtures (i.e., 0.41-0.8%VMA)
252 exhibited adequate repeatability, regardless of t_{rest} interval. Hence, the COV of various
253 responses determined by the vane varied from 5% to 7.5% and from 4.6% to 8.4% when
254 using direct shear. The COV that resulted from direct shear increased up to 11.7% and 15.4%
255 at t_0 for low and high thixotropic mixtures (i.e., 0.46-10%SF and 0.34-0.75%TEA,
256 respectively). For the former category of mixtures, the increased COV can be related to
257 reduced stability including bleeding and sedimentation, which affect variability of C
258 responses. In contrast, the increased COV resulting from high thixotropic mixtures can be
259 attributed to faster flocculation rates that make measurements quite sensitive to accuracy of
260 testing procedures.

261 **3-Effect of mortar composition on τ_0 and C**

262 The τ_0 measurements determined after mixing and 20 min later for tested mortars are plotted
263 in Fig. 6. As expected, mortars prepared with combinations of increased cement content and
264 reduced w/c led to higher τ_0 values, given the increased inter-particle links and reduced free
265 mixing water. For example, such increase at t_0 was from 39.4 to 53.2 and 63.3 Pa for the
266 0.46-5%SF, 0.41%-5%SF, and 0.34-5%SF, respectively. Also, for given w/c, τ_0 increased
267 with the addition of silica fume (due to increased packing density of matrix) or VMA (due to
268 polymer entanglement and hydrogen bonds) [2,3,7]. At longer elapsed resting times (i.e., at
269 t_{20}), all mortars exhibited increased τ_0 responses, depending on the flocculation rate
270 associated with cement hydration reactions that occurred during the rest period.

271 It is interesting to note that relatively low τ_0 values were determined right after mixing (i.e.,
272 at t_0) for mortars containing TEA, but then significantly increased over time. For example, τ_0
273 of 0.34-0.75%TEA was 50.3 Pa at t_0 , but reached the highest value of 1106 Pa at t_{20} . This
274 clearly reflects the thixotropic mode of action of this agent through which the physico-

275 chemical interactions of propylene carbonate with cement particles lead to significant
276 structural build-up at rest with increased τ_0 responses [17,18].

277 **Comparison with C values** – With the exception of 3 mortars made with 0.46-w/c possessing
278 unstable nature (i.e., 0.46-5%SF, 0.46-10%SF, and 0.46-0.35%VMA), the order of C
279 magnitude determined by direct shear at given t_{rest} was pretty close to that of corresponding τ_0
280 (Table 3); the measurements remained within the repeatability of testing. In the case of
281 unstable mortars, the C values determined after certain t_{rest} were higher by around 1.5 to 2.5
282 times than corresponding τ_0 . For instance, the C of 0.46-5%SF mortar registered after 20, 40,
283 and 60 min rest was 146, 363.5, and 612.7 Pa, respectively; while corresponding τ_0 was 85.7,
284 146.2, and 271 Pa, respectively. This could be related to reduced stability, including bleeding
285 and sedimentation that increase concentration of solid particles towards the lower half of the
286 shearing box where interfacial failure plane is expected to occur, thus leading to increased
287 shear stresses. The difference in material concentration was felt when trying to move a
288 spatula manually from the top surface to interfacial region in the shearing box [12].

289 The relationships between τ_0 and C responses for all tested mortars measured at various t_{rest}
290 along with their correlation coefficients (R^2) are given below (the relationships were forced to
291 intercept the origin of axis, thus having the form $y = A x$).

$$292 \quad \text{At } t_0: C = 1.104 \tau_0 \qquad R^2 = 0.82 \qquad \text{Eq. 4}$$

$$293 \quad \text{At } t_{20}: C = 0.964 \tau_0 \qquad R^2 = 0.92 \qquad \text{Eq. 5}$$

$$294 \quad \text{At } t_{40}: C = 0.905 \tau_0 \qquad R^2 = 0.97 \qquad \text{Eq. 6}$$

295 **4-The A_{Thix} values determined by different methods**

296 Typical example showing the determination of A_{Thix} by considering the slope of tendency
297 curves of τ_0 or (C value) determined at various t_{rest} using the vane or direct shear methods is
298 given in Fig. 7; the results obtained are summarized in Table 3. Clearly, the τ_0 and C values
299 followed increasing trends with resting time, depending on mortar constituents and ability to

300 restructure skeleton at rest. The R^2 of all tendency curves were higher than 0.95, reflecting
 301 that both methods can appropriately be used to assess A_{Thix} of cementitious materials.

302 The effect of CEM composition on $A_{\text{Thix}}(\tau_0)$ magnitudes is shown in Fig. 8. Following the
 303 same phenomena described earlier, $A_{\text{Thix}}(\tau_0)$ increased for mortars made with combinations
 304 of increased cement content and reduced w/c. For example, such increase was from 0.0682 to
 305 0.143 and 0.575 Pa/s for the 0.46-5%SF, 0.41%-5%SF, and 0.34-5%SF, respectively. Also,
 306 for given w/c, $A_{\text{Thix}}(\tau_0)$ increased with the addition of silica fume or VMA; at 0.41 w/c, this
 307 reached 0.178 and 0.892 Pa/s for 0.41-10%SF and 0.41-0.8%VMA, respectively. The highest
 308 $A_{\text{Thix}}(\tau_0)$ of 1.172 and 1.484 Pa/s corresponded to 0.34-w/c mortars made with 0.3% or 0.75%
 309 TEA, respectively, mostly related to the thixotropic nature of this agent.

310 **Comparison with $A_{\text{Thix}}(C)$ values** – As can be seen in Fig. 9, the ratio of $A_{\text{Thix}}(C)/A_{\text{Thix}}(\tau_0)$
 311 varied from 1.5 to 2.5 for the unstable 0.46-5%SF, 0.46-10%SF, and 0.46-0.35%VMA
 312 mortars. As previously explained, this can be related to reduced stability that over-estimated
 313 the shear stresses and resulted in higher $A_{\text{Thix}}(C)$. Subsequently, the $A_{\text{Thix}}(C)/A_{\text{Thix}}(\tau_0)$ ratio
 314 hovered around 1.0 for all other CEM, implying that the magnitude of A_{Thix} becomes almost
 315 similar for relatively stable mixtures, regardless of testing method. This reflects the accuracy
 316 of considering the slope of τ_0 determined at various t_{rest} to quantify the flocculation aspect of
 317 thixotropy, as well as its robustness as it is not affected by the testing method. The
 318 relationship between both indices for all tested mortars is given as:

$$319 \quad A_{\text{Thix}}(C) = 0.884 A_{\text{Thix}}(\tau_0) \quad R^2 = 0.97 \quad \text{Eq. 7}$$

320 The relationships between τ_0 or C responses determined after mixing (i.e., at t_0) and
 321 corresponding magnitude of A_{Thix} are plotted in Fig. 10. If excluding mortars prepared with
 322 TEA, it is interesting to note that τ_0 determined by the vane method can well be used to
 323 predict $A_{\text{Thix}}(\tau_0)$ with acceptable R^2 of 0.82. Mixtures containing TEA exhibited moderate τ_0
 324 values at t_0 , albeit their rates of increase were significantly accentuated. A relatively moderate

325 R^2 of 0.54 resulted from C determined by direct shear right after mixing and corresponding
326 $A_{\text{Thix}}(C)$ data.

327

SUMMARY AND CONCLUSIONS

328 Monitoring the flocculation aspect of thixotropy is essential to predict SCC properties after
329 casting such as stability, formwork pressure, and multi-layer interfaces. The main objective
330 of this paper is to evaluate the suitability of considering the evolution of τ_0 over time
331 determined by vane method in order to assess the magnitude of thixotropy. Three series of
332 highly flowable mortars are tested using a four-bladed vane, and results compared to C values
333 obtained by direct shear. Standardized under ASTM D3080 and available in most research
334 centers, the direct shear can be considered as a reference test to unify quantification and
335 validate constitutive models intended for yield behavior of cementitious materials.

336 Based on foregoing, test results have shown that τ_0 and C values increased when mixtures are
337 prepared with reduced w/c and/or addition of silica fume or VMA. The TEA led to
338 remarkably high τ_0 and C values, given the fast build-up of cementitious matrix. The
339 $A_{\text{Thix}}(C)/A_{\text{Thix}}(\tau_0)$ ratio varied from 1.5 to 2.5 for low thixotropic and unstable mortars, which
340 was attributed to bleeding and sedimentation that alter concentration of solid particles where
341 interfacial failure is expected to occur. In contrast, $A_{\text{Thix}}(C)/A_{\text{Thix}}(\tau_0)$ ratio hovered around 1.0
342 for stable mixtures, reflecting similar magnitudes of thixotropy. Adequate correlation exists
343 between thixotropy determined by four-bladed vane and direct shear methods. This reflects
344 the suitability of considering the slope of τ_0 determined at various rest intervals to quantify
345 thixotropy, as well as its robustness as it is not affected by the testing method.

346

REFERENCES

347 [1] Wallevik JE. Rheological properties of cement paste: Thixotropic behavior and structural
348 breakdown. Cement and Concrete Research. 2009; 39:14-29.

349 [2] RILEM Technical Committee, Final report of RILEM TC 188-CSC. Casting of self-

- 350 compacting concrete. *Materials and Structures*. 2006; 39:937-954.
- 351 [3] Assaad JJ, Khayat KH, Daczko J. Evaluation of static stability of self-consolidating
352 concrete. *ACI Materials Journal*. 2004; 101(3):168-176.
- 353 [4] Zhu W, Gibbs JC, Bartos PJM. Uniformity of in-situ-properties of self-compacting
354 concrete in full-scale structural elements. *Cement and Concrete Composites*. 2001; 23(1):57-
355 64.
- 356 [5] Assaad JJ, Khayat KH. Effect of coarse aggregate characteristics on lateral pressure
357 exerted by self-consolidating concrete. *ACI Materials Journal*. 2005; 102(3):145-153.
- 358 [6] Roussel N, Cussigh F. Distinct-layer casting of SCC: The mechanical consequences of
359 thixotropy. *Cement and Concrete Research*. 2008; 38:624-632.
- 360 [7] Assaad JJ, Issa C. Preliminary study on interfacial bond strength due to successive casting
361 lifts of self-consolidating concrete – Effect of thixotropy. *Construction and Building*
362 *Materials*. 2016; 126:351-360.
- 363 [8] Billberg P. Form pressure generated by self-compacting concrete – Influence of
364 thixotropy and structural behaviour at rest. Ph.D. thesis, Dep. of Structural Engineering, The
365 Royal Institute of Technology, Stockholm, 2006.
- 366 [9] Roussel N. Rheology of fresh concrete: from measurements to predictions of casting
367 processes. *Materials and Structures*. 2007; 40:1001-1012.
- 368 [10] Assaad JJ. Correlating thixotropy of self-consolidating concrete to stability, formwork
369 pressure, and multi-layers casting. *Journal of Materials in Civil Engineering*. 2016; 28(10)
370 DOI: 10.1061/(ASCE)MT.1943-5533.
- 371 [11] Nguyen QD, Boger DV. Direct yield stress measurement with the vane method. *Journal*
372 *of Rheology*. 1985; 29:335-347.
- 373 [12] Assaad JJ, Harb J, Maalouf Y. Measurement of yield stress of cement pastes using the
374 direct shear test. *Journal of Non-Newtonian Fluid Mechanics*. 2014; 214:18-27.

- 375 [13] ASTM D3080/D3080M-11. Standard Test Method for Direct Shear Test of Soils Under
376 Consolidated Drained Conditions. ASTM Internatinoal, West Conshohocken, PA, 2011.
- 377 [14] Barnes HA. A review of the slip (wall depletion) of polymer solutions, emulsions and
378 particle suspensions in viscometers; its cause, character, and cure. *Journal of Non-Newtonian*
379 *Fluid Mechanics*. 1995; 56:221-251.
- 380 [15] Alfani R, Guerrini GL. Rheological test methods for the characterisation of extrudable
381 cement-based materials – a review. *Materials and Structures*. 2005; 38:239-247.
- 382 [16] Lu G, Wang K. Theoretical and experimental study on shear behavior of fresh mortar.
383 *Cement and Concrete Composites*. 2011; 33:319-327.
- 384 [17] Assaad JJ, Daou Y. Cementitious grouts with adapted rheological properties for injection
385 by vacuum techniques. *Cement and Concrete Research*. 2014; 59:43-54.
- 386 [18] Khayat KH, Assaad JJ. Use of thixotropy-enhancing agent to reduce formwork pressure
387 exerted by self-consolidating concrete. *ACI Materials Journal*. 2008; 105(1):88-96.
- 388 [19] Schwartzentruber A, Catherine C. Method of the concrete equivalent mortar (CEM)—A
389 new tool to design concrete containing admixture. (in French), *Materials and Structures*.
390 2000; 33:475-482.
- 391 [20] Assaad JJ, Khayat KH. Assessment of thixotropy of self-consolidating concrete and
392 concrete-equivalent-mortar – Effect of binder composition and content. *ACI Materials*
393 *Journal*. 2004; 101(5):400-408.
- 394 [21] Assaad JJ, Harb J, Chakar E. Relationships between key ASTM test methods determined
395 on concrete and concrete-equivalent-mortar mixtures. *ASTM International Journal*. 2009;
396 6(3):1-14.
- 397
- 398
- 399

400
401

Table 1-Typical SCC classes and corresponding CEM composition

	Typical classes of SCC mixtures		
Cement, kg/m ³	375	435	500
w/c	0.46	0.41	0.34
Sand (0-4.75 mm), kg/m ³	970	935	920
Aggregates (1.18-9.5 mm), kg/m ³	825	795	780
Targeted slump flow, mm	650 ±20	650 ±20	650 ±20
	Tested mortars using the CEM approach		
Cement, kg/m ³	375	435	500
w/c	0.46	0.41	0.34
Sand (0-4.75 mm), kg/m ³	1065	1045	1010
Cement paste / sand, by volume	0.718	0.795	0.853
Silica fume, % of cement mass	0%, 5% and 10%		
VMA, % of cement mass	0%, 0.35%, and 0.8%		
TEA, % of cement mass	0%, 0.3%, and 0.75%		
HRWR, % of cement mass	Varies depending on CEM composition to achieve similar initial flow of 220 ±10 mm		

402
403
404

Table 2-Effect of mortar composition on HRWR demand and stability indices

	HRWR, % of cement	Initial flow, mm	Final set time, hr:min	Unit weight, kg/m ³	Flow time, sec	Bleeding	
						Bleed rate, %/min	Max. bleed, %
0.46-5%SF	0.62	225	9:30	1910	38.25	0.353	10.3
0.46-10%SF	0.65	220	10:15	1930	40.45	0.235	8.5
0.46-0.35%VMA	0.65	225	11:45	1915	48	0.267	8.3
0.46-0.8%VMA	0.77	225	14:15	1930	63.5	0.14	5
0.41-5%SF	0.8	220	11:45	2080	49	0.165	4.2
0.41-10%SF	0.86	225	13:00	2050	52.25	0.125	3.3
0.41-0.35%VMA	0.85	220	15:00	2040	59.5	0.13	3.1
0.41-0.8%VMA	0.95	230	16:45	2065	80.25	0.085	2.1
0.34-5%SF	1.12	225	14:45	2145	86.25	0.095	2.3
0.34-0.35%VMA	1.1	230	15:30	2160	90	0.065	1.5
0.34-0.3%TEA	1.05	225	12:15	2130	72.5	0.047	0.9
0.34-0.75%TEA	1.05	230	12:45	2135	74	0.03	0.5

405 Mixture codification refers to: w/c - Percent and type of additive used (i.e., silica fume,
406 VMA, or TEA)
407
408

409

410

Table 3-Determination of A_{Thix} by four-bladed vane and direct shear

	Four-bladed vane method		Direct shear method	
	t_{rest} (min) and corresponding τ_0 (Pa)	$A_{Thix}(\tau_0)$, Pa/s	t_{rest} (min) and corresponding C (Pa)	$A_{Thix}(C)$, Pa/s
0.46-5%SF	$t_0 = 39.4$; $t_{20} = 85.7$; $t_{40} = 146.2$; $t_{60} = 271$; and $t_{80} = 355.8$	0.0682	$t_0 = 45.1$; $t_{20} = 146$; $t_{40} = 363.5$; and $t_{60} = 612.7$	0.16
0.46-10%SF	$t_0 = 42.6$; $t_{20} = 79$; $t_{40} = 200.8$; $t_{60} = 284$; and $t_{80} = 418$	0.0796	$t_0 = 41.8$; $t_{20} = 162$; and $t_{40} = 382$	0.142
0.46-0.35%VMA	$t_0 = 36.7$; $t_{20} = 101.4$; $t_{40} = 273$; and $t_{80} = 522.6$	0.105	$t_0 = 38$; $t_{20} = 186$; and $t_{30} = 360.4$	0.171
0.46-0.8%VMA	$t_0 = 45$; $t_{20} = 273$; $t_{60} = 881$; and $t_{80} = 1264$	0.254	$t_0 = 39.8$; $t_{10} = 171$; and $t_{30} = 559$	0.293
0.41-5%SF	$t_0 = 53.2$; $t_{20} = 183.5$; $t_{40} = 383$; and $t_{80} = 725.6$	0.143	$t_0 = 49$; $t_{20} = 174.5$; $t_{40} = 386$; and $t_{60} = 556$	0.144
0.41-10%SF	$t_0 = 48.3$; $t_{20} = 206$; $t_{40} = 415$; and $t_{60} = 691.2$	0.178	$t_0 = 55$; $t_{20} = 188.6$; and $t_{40} = 426$	0.154
0.41-0.35%VMA	$t_0 = 57.6$; $t_{20} = 422.1$; $t_{40} = 682$; and $t_{60} = 1274$	0.326	$t_0 = 57.1$; $t_{10} = 359$; and $t_{30} = 732$	0.366
0.41-0.8%VMA	$t_0 = 61$; $t_{20} = 428$; $t_{40} = 1806$; $t_{60} = 2844$; and $t_{80} = 4206$	0.892	$t_0 = 57.2$; $t_{10} = 429$; and $t_{30} = 1517$	0.825
0.34-5%SF	$t_0 = 63.3$; $t_{40} = 1308$; $t_{60} = 1802$; and $t_{80} = 2947$	0.575	$t_0 = 64.7$; $t_{40} = 1022$; and $t_{60} = 1905$	0.495
0.34-0.35%VMA	$t_0 = 67.3$; $t_{20} = 493$; $t_{40} = 1482$; $t_{60} = 2734$; and $t_{80} = 4033$	0.848	$t_0 = 70.4$; $t_{20} = 620$; and $t_{50} = 2408$	0.796
0.34-0.3%TEA	$t_0 = 51.2$; $t_{20} = 769$; $t_{40} = 2275$; and $t_{60} = 4238$	1.172	$t_0 = 58.3$; $t_{10} = 566$; and $t_{30} = 1894$	1.032
0.34-0.75%TEA	$t_0 = 50.3$; $t_{20} = 1106$; $t_{40} = 3275$; and $t_{60} = 5266$	1.484	$t_0 = 49.7$; $t_{20} = 985$; and $t_{40} = 2995$	1.227

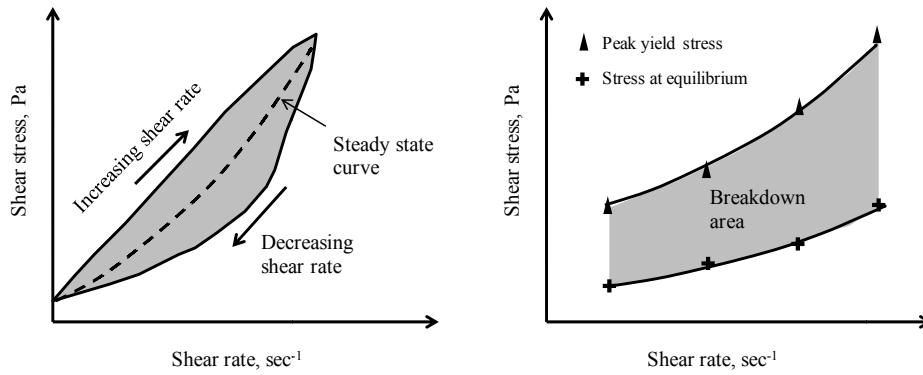
411

412

413

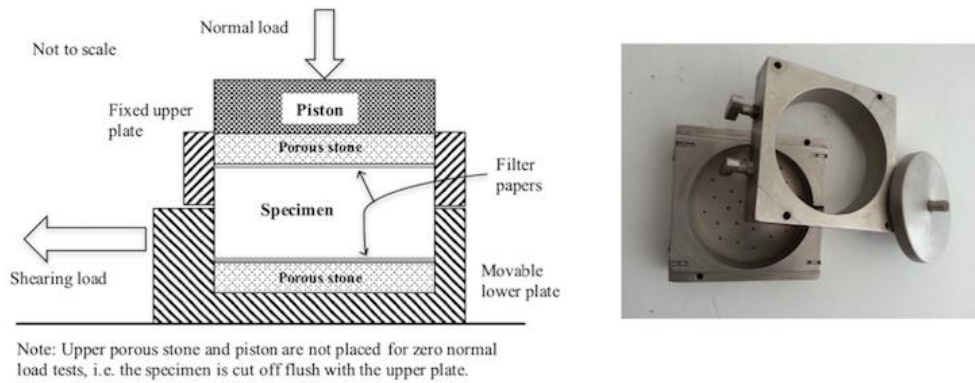
414

415



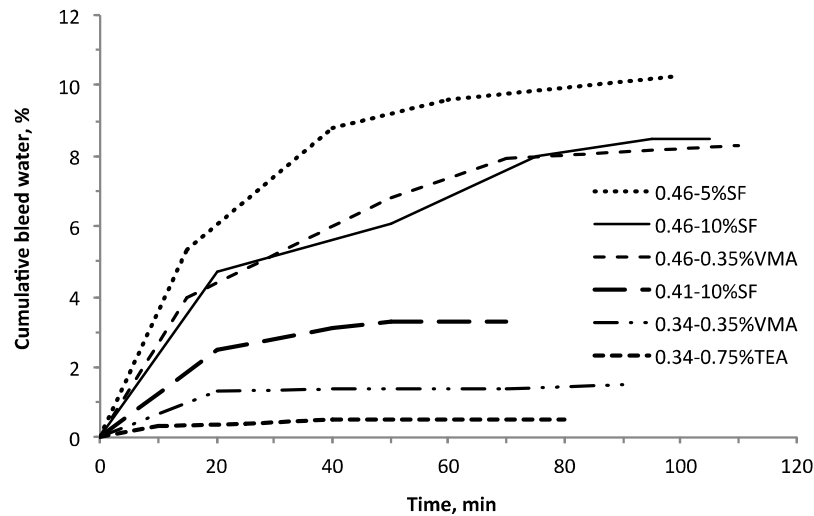
416
417
418
419
420
421
422

Fig. 1 Typical hysteresis loops and structural breakdown area for assessing the magnitude of thixotropy



423
424
425
426
427

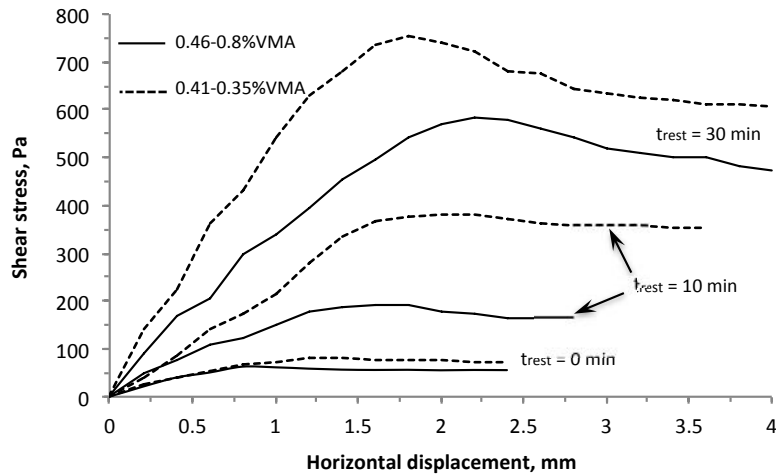
Fig. 2 Photo for direct shear test



428
429

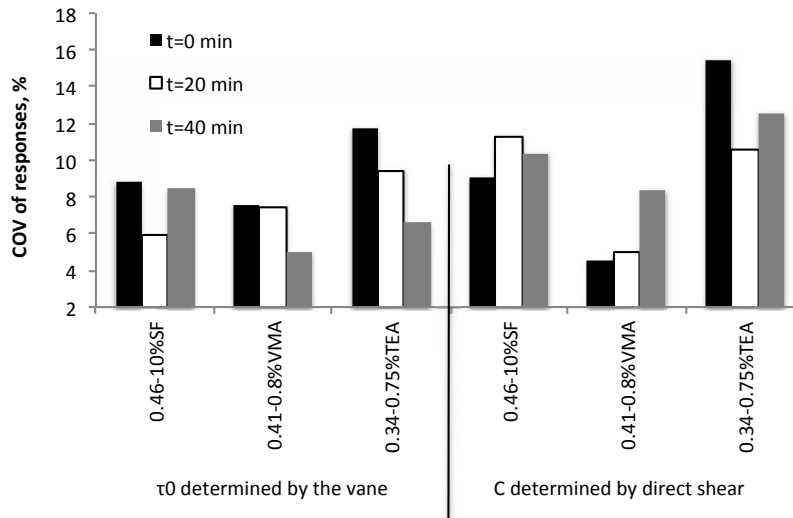
430
431
432
433

Fig. 3 Typical cumulative bleeding curves vs. time for selected mortars



434
435
436
437
438
439
440

Fig. 4 Typical shear stress vs. horizontal displacement plots determined at different t_{rest} by direct shear



441
442
443
444
445
446

Fig. 5 COV of τ_0 and C responses determined at different t_{rest}

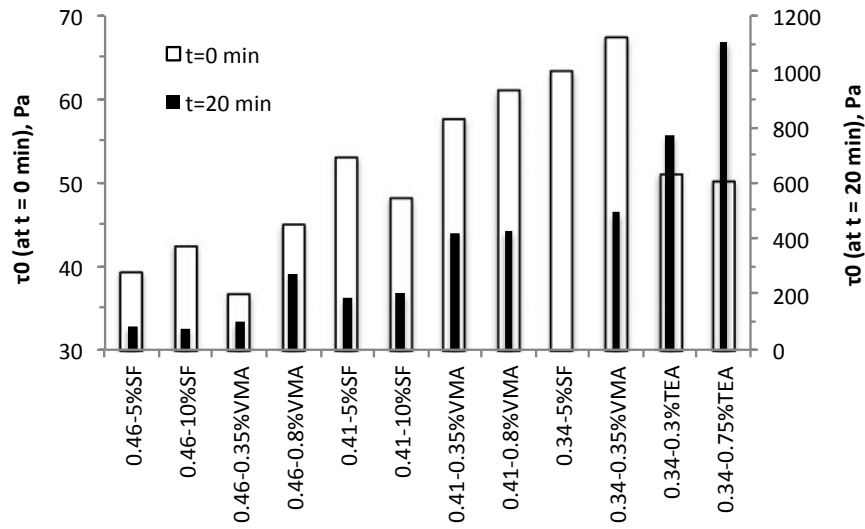


Fig. 6 Effect of mortar composition on τ_0 values determined at t_0 and t_{20}

447
448
449
450
451

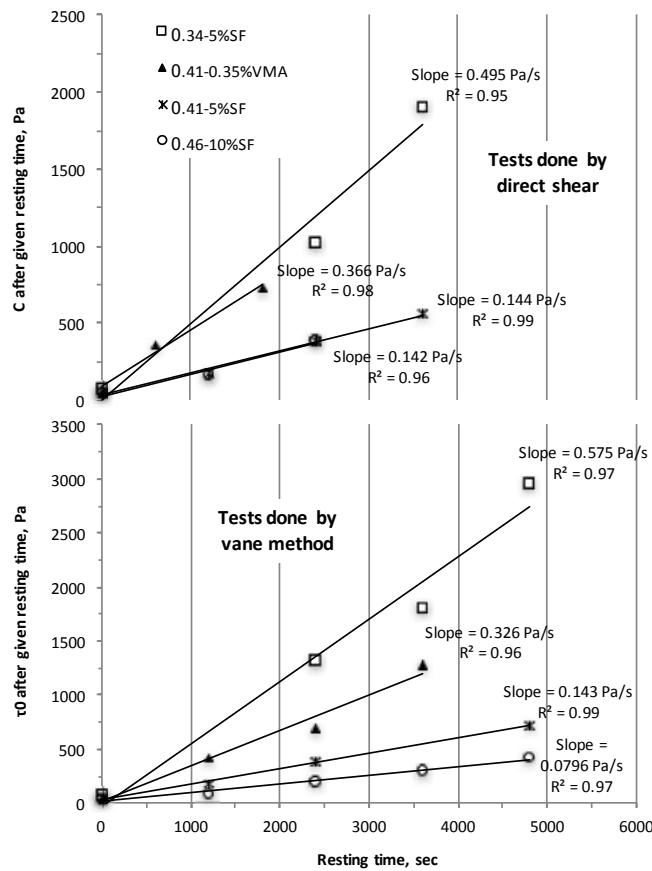


Fig. 7 Determination of $A_{Thix}(\tau_0)$ and $A_{Thix}(C)$ for selected mortars

452
453
454
455
456

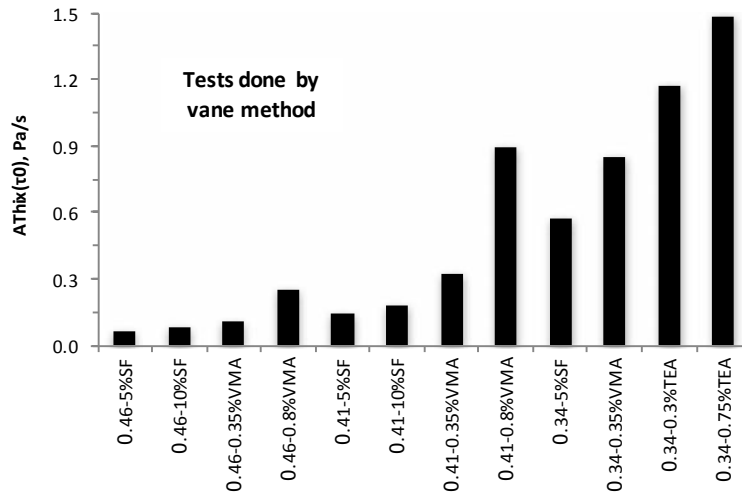


Fig. 8 Effect of mortar composition on $A_{Thix}(\tau_0)$ measurements

457
458
459
460
461

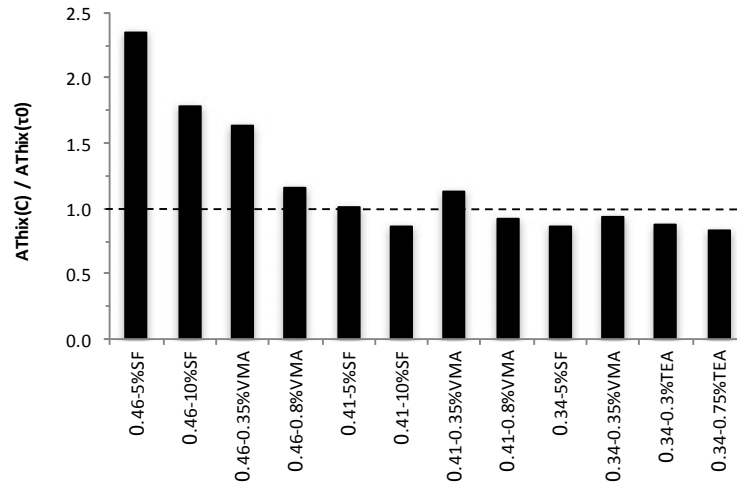
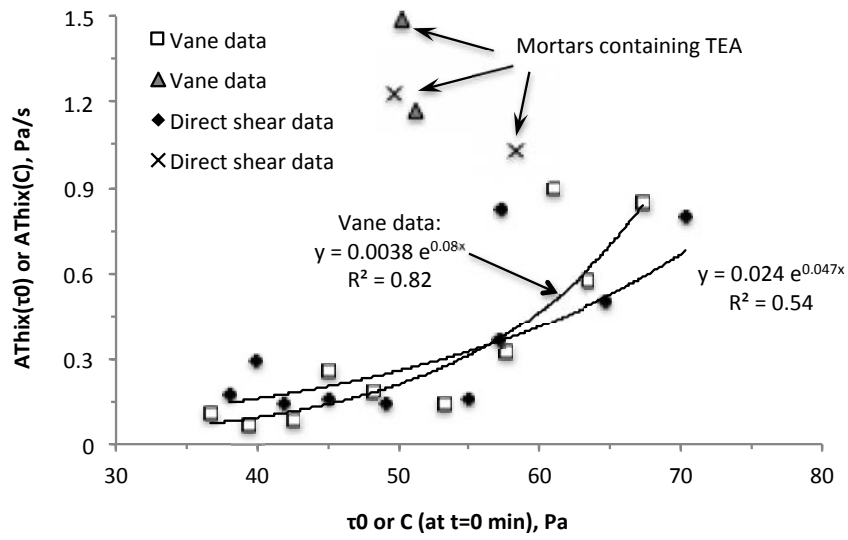


Fig. 9 Ratio between $A_{Thix}(C)$ and $A_{Thix}(\tau_0)$ measurements for tested mortars

462
463
464
465
466
467



468
469
470

Fig. 10 Prediction of $A_{Thix}(\tau_0)$ from τ_0 at t_0 (and $A_{Thix}(C)$ from C at t_0)